Journal of Intelligent & Fuzzy Systems 31 (2016) 2949–2957
DOI:10.3233/JIFS-169179
IOS Press

Active vibration adaptive fuzzy backstepping control of a 7-DOF dual-arm of humanoid robot with input saturation

Keqiang Bai[a,b,c,*], Minzhou Luo[a,b], Tao Li[d], Jue Wu[c,*], Lei Yang[c], Manlu Liu[a,c] and Guanwu Jiang[a,c]

[a]*Department of Automation, School of Information Science and Technology, University of Science and Technology of China, Hefei, P.R. China*

[b]*Institute of Intelligent Manufacturing Technology, Jiangsu Industrial Technology Research Institute, Nanjing, P.R. China*

[c]*Southwest University of Science and Technology, Mianyang, P.R. China*

[d]*Institute of Advanced Manufacturing Technology, Hefei Institutes of Physical Science, Chinese Academy of Sciences, Changzhou, P.R. China*

Abstract. This paper proposes a new controller based on the torque compensation method for the control of a 7-DOF dual-arm of a humanoid robot with input saturation residual vibration of the end-effector. Through theoretical and experimental analysis, an adaptive fuzzy backstepping control strategy was designed for the 7-DOF dual-arm control system. This strategy can be used to suppress the time-varying nonlinear residual vibration of the end-effector caused by inertia variations in the serial robot. Firstly, a boundary feedback controller was designed to asymptotically stabilize the closed-loop system based on the C_0-semigroup theory, which also proves the efficacy of the closed-loop system solution. Lyapunov stability analysis proved that the closed-loop demonstrated globally asymptotic stability. Secondly, an adaptive fuzzy backstepping method was designed for the dynamic compensator with a tracking filter for the control system of the 7-DOF dual-arm of the humanoid robot. The primary difference between this new method and conventional methods is that the new method does not require complex computation. In addition, this method improves the limit of computing power and memory space for the controllers. Finally, the effectiveness of the torque compensation strategy and the new method's ability to suppress the residual vibration are demonstrated via simulation and experiments.

Keywords: Torque compensation, 7-DOF dual-arm of humanoid robot, input saturation, adaptive fuzzy backstepping control

1. Introduction

With the development of robot technology, increasingly more hybrid robots are used in product lines to enhance productive efficiency. Examples include assembly robots [4], as well as robotic end-effectors, and transducers [1]; these robots are especially common in industries with heavy-load work, and in surgery. Faster robots with more precise motions are more productive. However, robot motions are often restricted by residual vibrations in the end-effector, which tend to be time varying and nonlinear due to configuration dependent friction, inertia variation, and nonlinear joint stiffness [9]. Researchers have proposed various methods to suppress residual vibration. Currently, there are two distinct modifications:

*Corresponding author. Keqiang Bai, Department of Automation, School of Information Science and Technology, University of Science and Technology of China, Hefei 230026, China. Tel./Fax: +86 15983658733; E-mail: baisir@mail.ustc.edu.cn. (K. Bai); Jue Wu, Southwest University of Science and Technology, Mianyang 621010, China. E-mail: wujue@aliyun.com. (J. Wu).

mechanical structure modifications and control algorithm or strategy modifications.

For the first scheme, mechanical modification can improve vibration suppression; the mechanical design corresponds to the specific application, which may limit the flexibility of the robot. The latter scheme is primarily based on the closed-loop backward control system. Apart from the control methods, the semi-group theory proposes stability analysis and uniqueness. Lou et al. [6], a hybrid proportional-differential (PD) and effective multi-mode positive position feedback control controller were proposed to suppress vibrations by effective multi-mode positive position feedback and the use of a derivative controller to realize motion control. Although disturbance is considered, two control schemes, the active disturbance rejection control (ADRC) and sliding mode control (SMC) approaches were adopted for the use of a single-dimensional Euler-Bernoulli equation, in which the closed-loop system is asymptotically stable [2]. Lou et al. [6] and Guo et al. [2] proposed that it is possible to design a controller based on the semi-group theory for the single-link flexible manipulator system, which demonstrates the effectiveness of the semi-group theory.

The problem of vibration suppression and input saturation in the dual-arm cooperation of a humanoid robot system were investigated by Ge et al. [12] and He et al. [13] considered the flexible string lateral vibration of the system, so a secondary system was introduced to deal with the problem of input saturation. However, since the dual-arm cooperation of humanoid robots cannot be accurately modeled, precise control and vibration reduction are lacking. An alternative to the backstepping holonomic tracking method was presented by Huang et al. [5]. The algorithm employed hybrid intelligent fuzzy system Taguchi ant colony optimization (FS-TACO) with dynamic tracking control of three-wheeled holonomic mobile robots. Tong et al. [10, 11] and Karagiannis [3] focused on the adaptive fuzzy backstepping control of nonlinear systems. An alternative to the adaptive backstepping method (AAB) was presented by Karagiannis [3]. Xiao, et al. [14] proposed that an adaptive sliding mode controller was investigated by using the online updating law for a flexible spacecraft with partial loss of the actuator effectiveness fault.

However, implementing this algorithm requires complex computation for torque estimation due to the nonlinearity of the serial robot control system. In this paper, a tracking filter is considered for the control system of a 7-DOF dual-arm of a humanoid robot with input saturation, and a boundary feedback controller is proposed to stabilize the system. Switching laws are also designed to track angular velocity depending on angular velocity tracking errors; the joint torque is computed based on the dynamic model of the robot.

This paper is organized as follows. Section 2 presents preliminaries and problem formulation. Section 3 presents control law design and stability analysis and compensator with tracking filter. Section 4 presents our simulation and an experiment of the robot manipulator with input saturation. Section 5 presents the conclusions.

2. Preliminaries and problem formulation

Consider a class of single input-single output nonlinear systems which can be turned into one-half of a strict feedback form with known smooth and continuous functions and input saturations. The dynamic equation of the system can be expressed as follows:

$$\begin{cases} \dot{x}_i = x_{i+1} + \phi_i^T(x_1, x_2, \cdots, x_i) \\ \quad \theta_i, i = 1, 2, \cdots, n-1, \\ x_n = \tau + \phi_n^T(x_1, x_2, \cdots, x_i)\theta_n, \\ y = x_1 \end{cases} \tag{1}$$

where $x = [x_1, x_2, \cdots, x_n]^T$ denotes the system state variable, and $\phi_i(x_i)$ are known nonlinear smooth functions; $\phi_i(0, 0, \cdots, 0) = 0; \theta = [\theta_1, \cdots, \theta_p]^T \in R^p$ is an unknown constant vector; and τ and y are the follower input and output, respectively.

The control objective is to design a boundary control to suppress the transverse vibrations of the end-effector system of the 7-DOF dual-arm of a humanoid robot. Saturation nonlinearity in the maximum and minimum operational limits of the 7-DOF dual-arm of a humanoid robot system are unavoidable.

The input saturation is expressed as follows [7]:

$$\tau'(t) = \begin{cases} \operatorname{sgn}(\tau_0'(t))\tau_0'; & \left|\tau_0'(t)\right| \geq \tau'_{\max} \\ \tau_0'(t); & \left|\tau_0'(t)\right| < \tau'_{\max} \end{cases} \tag{2}$$

where $\tau_0'(t)$ is the designed control input, $\tau'(t)$ is the desired control input, and $\tau'_{\max}$ is the upper boundary of the saturation input $\tau'(t)$.

Figure 1 shows the hyperbolic tangent function of the saturation function approximation.

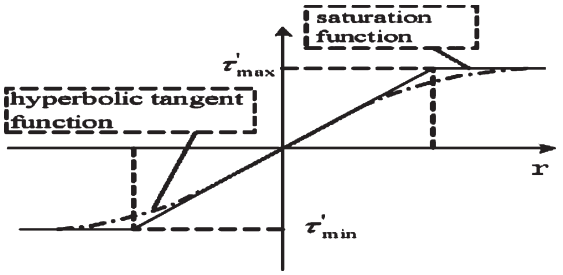

Fig. 1. Symmetric saturation nonlinearity and the hyperbolic tangent function.

The dynamic equation of the robot arm can be expressed as follows:

$$\begin{aligned} &\boldsymbol{M}_i(\boldsymbol{q}_i, m_0)\ddot{\boldsymbol{q}}_i + \boldsymbol{C}_i(\boldsymbol{q}_i, \dot{\boldsymbol{q}}_i, m_0)\dot{\boldsymbol{q}}_i \\ &\quad + \boldsymbol{F}_i(\boldsymbol{q}_i, \dot{m}_0)\dot{\boldsymbol{q}}_i + \boldsymbol{G}_i(\boldsymbol{q}_i, m_0) = \boldsymbol{\tau}_i \\ &\boldsymbol{y} = \boldsymbol{q} \end{aligned} \tag{3}$$

where $\boldsymbol{M}_i(\boldsymbol{q}_i, m_0)$ is the symmetric positive definite and the bounded inertial matrix of the robotic arm. $\boldsymbol{C}_i(\boldsymbol{q}_i, \dot{\boldsymbol{q}}_i, m_0)$ is the Coriolis and centrifugal matrix, $\boldsymbol{F}_i(\boldsymbol{q}_i, \dot{m}_0)$ is the additional item in the load time-varying parameters, $\boldsymbol{G}_i(\boldsymbol{q}_i, m_0)$ is the gravitational force vector, $\boldsymbol{\tau}_i$ is the control vector, and $\boldsymbol{y} \in \boldsymbol{R}^n$ is the output vector.

The simplification can be expressed as follows:

$$\begin{aligned} &\boldsymbol{M}(\boldsymbol{q}, m_0)\ddot{\boldsymbol{q}} + \boldsymbol{C}(\boldsymbol{q}, \dot{\boldsymbol{q}}, m_0)\dot{\boldsymbol{q}} \\ &\quad + \boldsymbol{F}(\boldsymbol{q}, \dot{m}_0)\dot{\boldsymbol{q}} + \boldsymbol{G}(\boldsymbol{q}, m_0) = \boldsymbol{\tau} \\ &\boldsymbol{y} = \boldsymbol{q} \end{aligned} \tag{4}$$

This paper makes the following assumptions:

Assumption 1. There exists $k_i(x_1, \cdots, \chi) > k_i > 0$, such that $\frac{\partial \beta_i}{\partial x_j} = \delta_{ij}(x_1, \cdots, x_i)\phi_i(x_1, \cdots, x_i)$, $j = 1, \cdots, i-1$ where $\delta_{ij}(x_1, \cdots, x_i)$ is a bounded function, $\left|\delta_{ij}(x_1, \cdots, x_i)\right| \le m_{ij}, m_{ij} > 0$.

3. Control law design and stability analysis and compensator with tracking filter

3.1. Adaptive fuzzy backstepping control law design

Let $\boldsymbol{x}_1 = \boldsymbol{q}, \boldsymbol{x}_2 = \dot{\boldsymbol{q}}$. The vibration suppression for the robot is derived by using adaptive fuzzy backstepping methods and a system described as follows:

$$\begin{aligned} \dot{\boldsymbol{x}}_1 &= \boldsymbol{x}_2 \\ \dot{\boldsymbol{x}}_2 &= \boldsymbol{x}_3 + \boldsymbol{\phi}_2(\boldsymbol{x}_1, \boldsymbol{x}_2)^T\boldsymbol{\theta}_2 + \boldsymbol{f}_2(\boldsymbol{x}_2) \\ \dot{\boldsymbol{x}}_3 &= \frac{1}{\mathrm{T}}\boldsymbol{\tau} - \frac{1}{\mathrm{T}}\boldsymbol{x}_3 \end{aligned} \tag{5}$$

where $\boldsymbol{x}_1, \boldsymbol{x}_2, \boldsymbol{x}_3$ denote the angle of the mechanical arm, angular velocity, and deflection angle at the end-effector, respectively; T denotes the time constant of the end-effector; $\boldsymbol{\tau}$ denotes the control input of the system; $\boldsymbol{\theta}_2 \in \boldsymbol{R}^5$ denotes the unknown parameter vector; and $\boldsymbol{\phi}_2(\boldsymbol{x}_1, \boldsymbol{x}_2)^T = [1, \boldsymbol{x}_1, \boldsymbol{x}_2, |\boldsymbol{x}_1|\boldsymbol{x}_2, |\boldsymbol{x}_2|\boldsymbol{x}_2]$ is a known smooth and continuous function.

The definition of the dynamic surface error $\boldsymbol{e}_1 = \boldsymbol{x}_1 - \alpha_0, \alpha_0 = y_d$ can be obtained as follows:

$$\dot{\boldsymbol{e}}_1 = \dot{\boldsymbol{x}}_1 - \dot{\boldsymbol{y}}_d \tag{6}$$

Virtual control items are introduced to the controller

$$\boldsymbol{\alpha}_1 = -\lambda_1\boldsymbol{e}_1 \tag{7}$$

where $\lambda_1 > 0$.

Let $\boldsymbol{\alpha}_1$ be the input control and z_2 represent the error state variables; a first-order filter can be obtained as follows:

$$\boldsymbol{\alpha}_1 = k\dot{z}_2 + z_2 \tag{8}$$

where k has been designed for the constant.

Step 2. The second subsystem of system (5) is $\dot{\boldsymbol{x}}_2 = \boldsymbol{x}_3 + \boldsymbol{\phi}_2(\boldsymbol{x}_1, \boldsymbol{x}_2)^T\boldsymbol{\theta}_2 + \boldsymbol{f}_2(\boldsymbol{x}_2)$. The definition of the second dynamic surface error is $\boldsymbol{e}_2 = \boldsymbol{x}_2 - z_2$.

$$\dot{\boldsymbol{e}}_2 = \dot{\boldsymbol{x}}_2 - \dot{z}_2 = \boldsymbol{x}_3 + \boldsymbol{\phi}_2(\boldsymbol{x}_1, \boldsymbol{x}_2)^T\boldsymbol{\theta}_2 + \boldsymbol{f}_2(\boldsymbol{x}_2) - \dot{z}_2 \tag{9}$$

The virtual control items are introduced to the controller

$$\boldsymbol{\alpha}_2 = u_{F2} + \dot{\alpha}_1 \tag{10}$$

where $u_{F2} = -\lambda_2\boldsymbol{e}_2 - \boldsymbol{e}_1 - \hat{\boldsymbol{f}}_{\alpha 2}(x_2) + \boldsymbol{\phi}_2(\boldsymbol{x}_1, \boldsymbol{x}_2)^T(\hat{\boldsymbol{\theta}}_2 + \boldsymbol{\beta}_2)$ $\hat{\boldsymbol{f}}_{\alpha 2}(x_2) = \hat{\boldsymbol{\Phi}}_2^T\boldsymbol{P}(x_2)$ is the fuzzy system close to $f_{\alpha 2}(x_2) = f_2(x_2) - \dot{\alpha}_1$.

The parameter adaptive law for

$$\dot{\boldsymbol{\theta}}_2 = -\frac{\partial \boldsymbol{\beta}_2}{\partial x_1}x_2 - \frac{\partial \boldsymbol{\beta}_2}{\partial x_2}[x_3 + \boldsymbol{\phi}_2(\boldsymbol{x}_1, \boldsymbol{x}_2)^T(\hat{\boldsymbol{\theta}}_2 + \boldsymbol{\beta}_2)] \tag{11}$$

$$\dot{\hat{\boldsymbol{\Phi}}}_2 = k_2 e_2 \boldsymbol{P}_2(x_2)$$

where

$$\boldsymbol{\beta}_2 = \int_0^{x_2} \kappa \boldsymbol{\phi}_2(x_1, \chi) d\chi = \kappa \left[x_2, x_1 x_2, \frac{1}{2}x_2^2, \frac{1}{2}|x_1|x_2^2, \frac{1}{3}|x_2|x_2^2 \right]^T.$$

The system actual control law for

$$\boldsymbol{\tau} = u_{F3} + \mathrm{T}\left(-k_3 \boldsymbol{e}_3 - \boldsymbol{e}_2 + \frac{1}{\mathrm{T}}x_3 + \dot{x}_{3f}\right) \quad (12)$$

where, $u_{F3} = -\lambda_3 \boldsymbol{e}_3 - \boldsymbol{e}_2 - \hat{\boldsymbol{f}}_{\alpha 3}(x_3)$ $\hat{\boldsymbol{f}}_{\alpha 3}(x_3) = \hat{\boldsymbol{\Phi}}_3^T \boldsymbol{P}(x_3)$ is the fuzzy system $f_{\alpha 3}(x_3) = f_3(x_3) - \dot{\alpha}_2$.

3.2. Stability analysis

In this paper, the model for the 7-DOF dual-arm of the humanoid robot system with input saturation was built as an Euler-Bernoulli beam model with five ordinary differential equations (ODEs) and one partial differential equation (PDE) obtained by Hamilton's principle, considering the disturbance of the tip payload. As shown in Fig. 2, $w(x,\ t)$ is the elastic deflection at position x for time t in the X_1OY_1 coordinate system; μ is the sum of the angular displacement; $y(x,\ t)$ is the displacement at position x for time t in the XOY coordinate system; $d(t)$ is the unknown disturbance on the end-effector load; and $\tau'(t)$ is the boundary feedback control on the left boundary. Considering the small vibrations of the flexible arm system, the angular rotation and the elastic deflection are so small that the following equation can be approximately obtained:

$$y(x, t) = x\mu(t) + w(x, t) \quad (13)$$

The kinetic energy of the robotic single-arm system $E_k(t)$ can be described as follows:

$$E_k(t) = \frac{1}{2}I_h\theta_t^2(t) + \frac{1}{2}\rho\int_0^L [y_t(x, t)]^2 dx + \frac{1}{2}m[y_t(L, t)]^2 \quad (14)$$

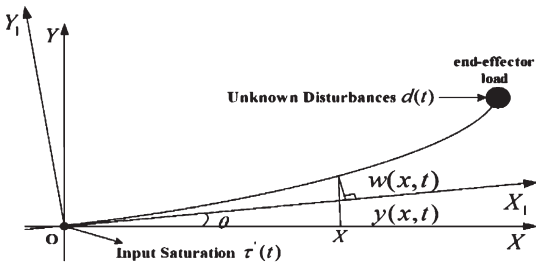

Fig. 2. Terminology of the mechanical arm.

where L is the length of the single-arm humanoid robot, m is mass of the robotic arm payload, I_h is the inertia of the hub, ρ is the uniform mass per-unit length of the humanoid robot mechanical arm, and $\theta(t)$ is angular position of the hub.1

The potential energy E_p can be obtained as follows:

$$E_p(t) = \frac{1}{2}EI\int_0^L [w_{xx}(x, t)]^2 dx + \frac{1}{2}T\int_0^L [w_x(x, t)]^2 dx \quad (15)$$

where EI is the bending stiffness of the single-arm humanoid robot.

The virtual work of the disturbance is given by Formula (16), as follows:

$$\delta W_f = d(t)\delta\theta(t) \quad (16)$$

The virtual work done by the boundary control $\tau(t)$ is written as follows:

$$\delta W_m = \tau'(t)\delta\theta(t) \quad (17)$$

Then, the total virtual work done on the system is expressed as follows:

$$\delta W = \delta W_f + \delta W_m \quad (18)$$

By using Hamilton's principle such that

$$\int_{t_1}^{t_2} \delta[E_k(t) - E_p(t) + W(t)]dt = 0 \quad (19)$$

the governing equation of the single-arm humanoid robot system is obtained as follows:

$$\rho y_{tt}(x, t) = -EIy_{xxxx}(x, t) + Ty_{xx}(x, t)$$
$$\forall (x, t) \in (0, L) \times [0, \infty),\ t \in [0, \infty) \quad (20)$$

The system boundary conditions can be described as follows:

$$\begin{cases} w(0, t) = 0, \\ w_x(0, t) = 0, \\ w_{xx}(L, t) = 0, \\ my_{tt}(L, t) = EIy_{xxx}(L, t) - Tw_x(L, t) \end{cases} \quad (21)$$

An observer $\hat{d}(t)$ is designed as the estimated value of the disturbance $d(t)$ in the dual-arm of a humanoid robot system, converging exponentially as follows:

$$\begin{cases} \zeta_t(t) = -k_1\tau_1' - k_1\hat{d} - kk_1\eta_t(t) \\ \hat{d} = \zeta(t) + k_1\eta_t(t) \end{cases} \quad (22)$$

where k is a positive constant and $\tau_1'(t)$ is one part of the saturation input $\tau'(t)$ designed according to the following text.

Thus,

$$\zeta_t(t) = -k_1\tau_1' - kk_1\eta_t(t) - k_1[\zeta(t) + k_1\eta_t(t)] \quad (23)$$

$$\tilde{d}_t(t) = -\hat{d}(t) = -\zeta_t(t) - k_1\eta_{tt}(t)] \quad (24)$$

where $\tilde{d}(t) = d(t) - \hat{d}(t)$.

The boundary control Lyapunov function is designed as follows:

$$V(t) = V_1(t) + V_2(t) + V_3(t) \quad (25)$$

Taking

$$\begin{aligned} V_1(t) &= \frac{\gamma k_1}{2}\rho\int_0^L y_t^2(x,t)dx \\ &\quad + \frac{\gamma k_1}{2}EI\int_0^L y_{xx}^2(x,t)dx \\ &\quad + \frac{\gamma k_1}{2}T\int_0^L w_x^2(x,t)dx + \frac{\gamma k_1}{2}my_t^2(L,t) \\ V_2(t) &= \frac{k_1}{2}\varphi_t^2(t) \\ V_3(t) &= \sigma\ln(\cosh(k_1\psi(t) + k_2\psi_t(t))) \\ &\quad + \varsigma\ln(\cosh(k_2\psi_t(t)) + \frac{1}{2}\tilde{d}^2(t) \end{aligned} \quad (26)$$

where $\psi_t(t) = y_{xt}(0,t) + k_2w(L,t) - k_1y_{xx}(0,t)$.

Lemma 1. *$V(t)$ is a positive definite when a humanoid robot-plus-manipulated object system is at equilibrium, $V(t) = 0$;*

Proof. When a humanoid robot-plus-manipulated object system is at an equilibrium, it can be obtained that: $w(x,t_0) = 0$; $y(x,t_0) = 0$; $\forall x \in [0, L]$. Thus, $V_1(t) = V_2(t) = V_3(t) = 0$, namely, $V(t) = 0$. When $t \neq t_0$, $V_1(t) \geq 0$, $V_2(t) \geq 0$, $V_3(t) \geq 0$. It is noted that V_1, V_2 and V_3 cannot simultaneously equal zero. Therefore, $V(t) > 0$ for $t \neq t_0$.

Lemma 2. *$\dot{V}(t)$ is negative. Since the disturbance observer converges exponentially, there exists a limited time t_{k_1} with $|\tilde{d}(t)| \leq k_1$, for $\forall k_1 > 0$.*

When $t \to \infty$, $\tilde{d}(t) \to 0$, the closed-loop boundary is asymptotically stable in the input saturation system.

The system's Lyapunov function can be described as follows:

$$V = V_{n-1} + \frac{1}{2}e_n^2 + \frac{1}{2\eta_n}\tilde{\boldsymbol{\Phi}}^T\tilde{\boldsymbol{\Phi}} \quad (27)$$

$$\begin{aligned} \dot{V} &= \dot{V}_{n-1} + e_n^2 - \frac{1}{\eta_n}\tilde{\boldsymbol{\Phi}}^T\dot{\hat{\boldsymbol{\Phi}}} \\ &\leq -\sum_{j=1}^{n-1}(\lambda_j - \frac{1}{2})e_j^2 + e_{n-1}e_n + \sum_{j=1}^{n-1}\varepsilon_j \\ &\quad + e_n(\tau + f_n(x_n) - \dot{\alpha}_{n-1}) - \frac{1}{\eta_n}\tilde{\boldsymbol{\Phi}}^T\dot{\hat{\boldsymbol{\Phi}}} \end{aligned} \quad (28)$$

Next, substitute the actual controller (12) and parameter adaptive law (11) into Equation (28) to obtain the following:

$$\dot{V} \leq -\sum_{j=1}^{n}(\lambda_j - \frac{1}{2})e_j^2 + \sum_{j=1}^{n-1}\varepsilon_j \quad (29)$$

In which, the design of constant $\lambda_j > 0.5$, $\varepsilon_j = \sigma_j^2 + 0.2785\varphi_j$, $j = 1, 2, 3$. Suppose $\varepsilon_0 = \sum_{j=1}^{3}\varepsilon_j$; considering the approximation error of the fuzzy system a boundedness, $\varepsilon_0 > 0$ and bounded. Suppose $\lambda_0 = \min\{(\lambda_1 - 0.5), (\lambda_2 - 0.5), (\lambda_3 - 0.5)\}$, therefore, Equation (29) is modified as follows:

$$\dot{V} \leq -\lambda_0\sum_{j=1}^{3}e_j^2 + \varepsilon_0 \quad (30)$$

Equation (30) is integrated into $t \in [0,\ T]$ to obtain the following:

$$V(T) - V(0) \leq -\lambda_0\int_0^T\sum_{j=1}^{3}e_i^2dt + \int_0^T\varepsilon_0dt \quad (31)$$

Considering $V(T) \geq 0$, Equation (31) is modified as follows:

$$\int_0^T\sum_{j=1}^{3}e_i^2dt \leq \frac{1}{\lambda_0}V(0) + \frac{1}{\lambda_0}\int_0^T\varepsilon_0dt \quad (32)$$

To achieve control objectives, assume that the input command y_d and its two derivatives exist and are bounded.

3.3. Torque compensation strategy of tracking filter

To suppress nonlinear and time-varying residual vibrations in the 7-DOF dual-arm of a humanoid robot, torque compensation methods are proposed to calculate the parameters of real-time torque using data from the previous servo cycle. As a result, applying torque compensation becomes more convenient because the torque parameters for this method can be acquired. Figure 3 shows the schematic diagram of

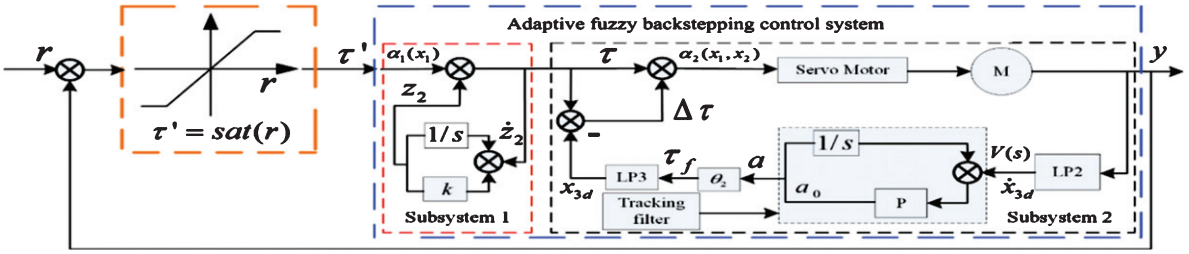

Fig. 3. The framework of the control system.

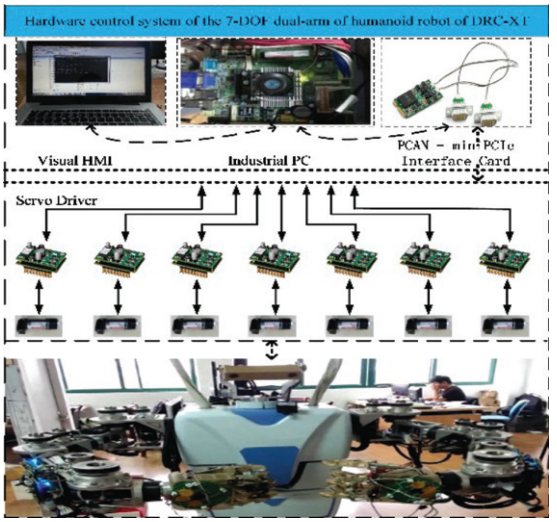

Fig. 4. The structure of the robot hardware control system.

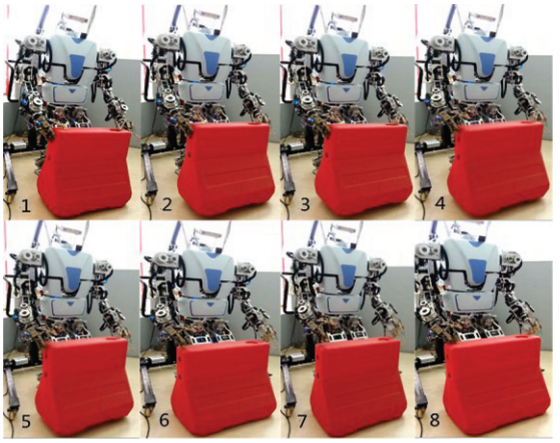

Fig. 5. The noumenon of the 7-DOF robot arm motion test process.

the control system. Detailed compensation strategy please reference [8].

4. Simulation and Experiment

To verify the proposed algorithm, an application in the 7-DOF dual-arm of the humanoid robot control system is presented to analyze the working process of the algorithm.

4.1. Hardware control system and experiment

As shown in Fig. 4, the system was composed of the visual HMI, Industrial PC, PCAN – mini PCIe interface card, servo system, and the humanoid robot noumenon. All functions, such as visual teaching and site monitoring, can operate via this HMI. An industrial PC can be used to implement the varied motion computations, such as the kinematics and inverse kinematics for the robot trajectory.

To demonstrate the validity of the proposed control method, an experiment was conducted on a dual-arm robot. As shown in Fig. 5. The dual-arm robot has 14 degrees of freedom, and every wrist joint has been equipped with a 6D-force sensor. The manipulated object is a plastic box, weighting 2000 g. Figure 5 depicts the experimental system process between the fingers and objects at the contact spot; there is no relative movement between the ends of the fingers and the objects. The first image represents the initial state wherein the robot arms are only influenced by their own weight. The two arms must lift the object. Images 2–5 depict an example of a system that is likely chattering under input saturation. To prevent vibration, data was recorded with 6D-force sensors.

4.2. Simulation and experiment result

The simulation system is described as follows:

$$\begin{cases} \dot{x}_1 = x_2 \\ \dot{x}_2 = \dfrac{K_t}{M_t} x_3 - \dfrac{B}{M_t} x_2 + \dfrac{N}{M_t} \sin(x_1) + d_2(x,t) \\ \dot{x}_3 = -\dfrac{R}{L} x_3 - \dfrac{K_b}{L} x_2 + \dfrac{1}{L} u - \dfrac{1}{L} d_3(x,t) \end{cases}$$

where x_1, x_2, x_3 and u denote the mechanical arm position, velocity, and electric current of the motor and input of the system, respectively; $y = x_1$ is the system output; $d_2(x, t)$ denotes parameter uncertainty; and $d_3(x, t) = 4\sin(t)$ denotes parameter uncertainty and external disturbance.

Figure 6 shows the fuzzy system robust adaptive back-stepping control system simulation. Figure 6(a)

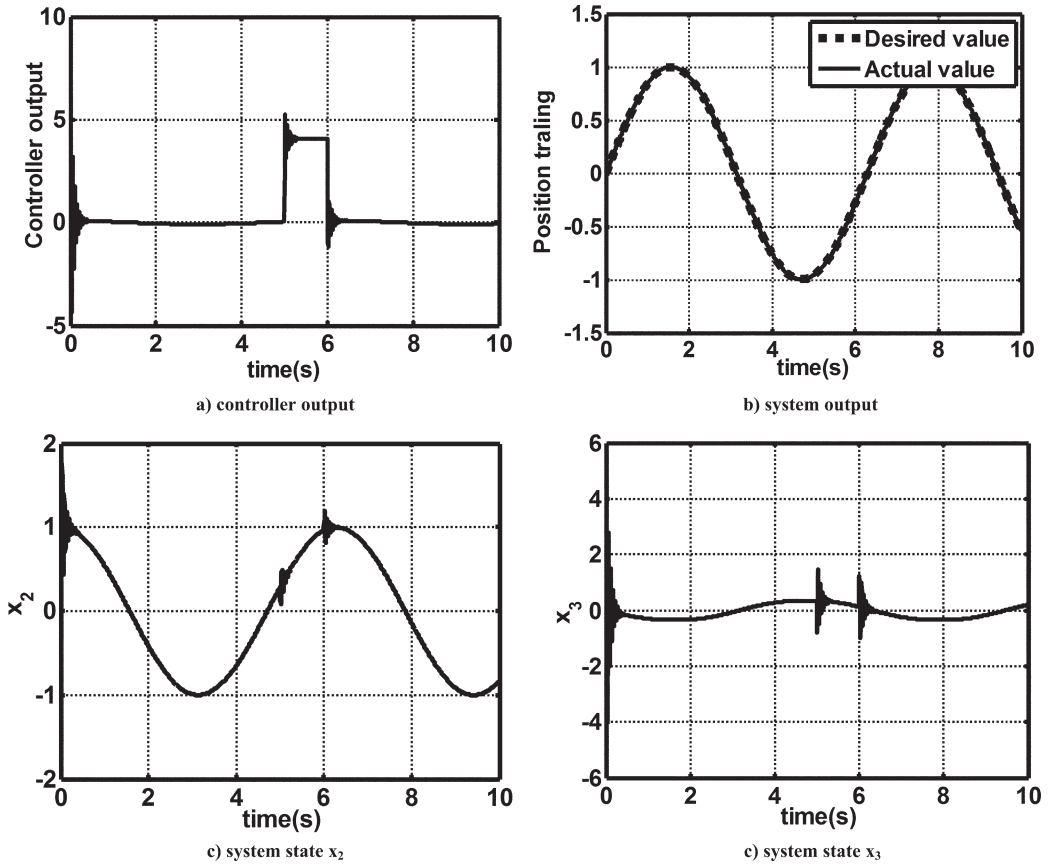

Fig. 6. Based on the fuzzy system robust adaptive backstepping control system simulation.

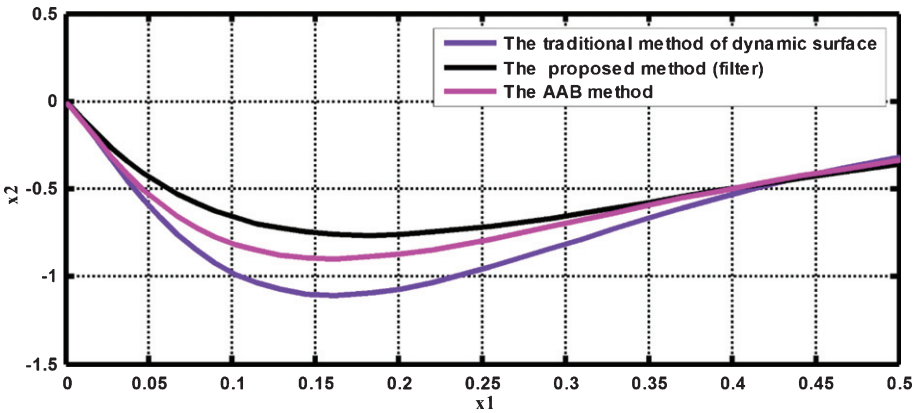

Fig. 7. The x1-x2 phase plane of the system dynamic response.

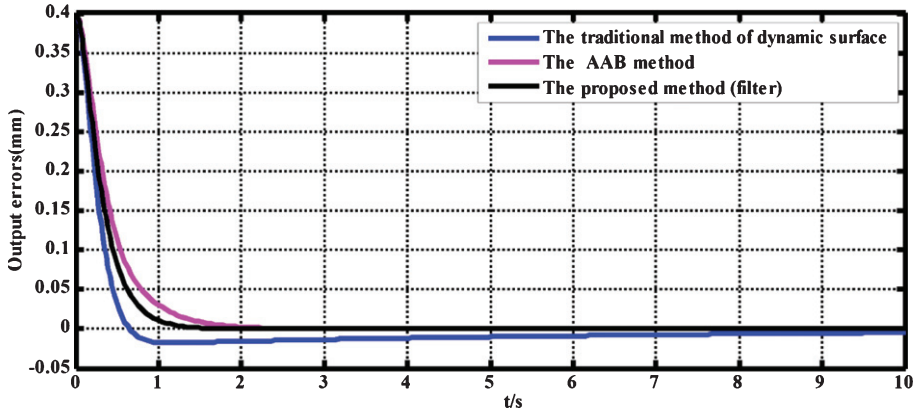

Fig. 8. The system output response.

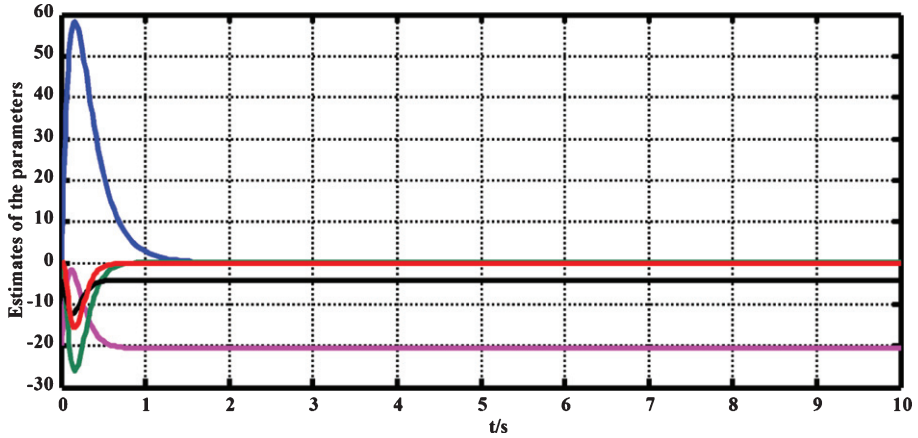

Fig. 9. Estimates of the parameters of $\hat{\theta}_2$.

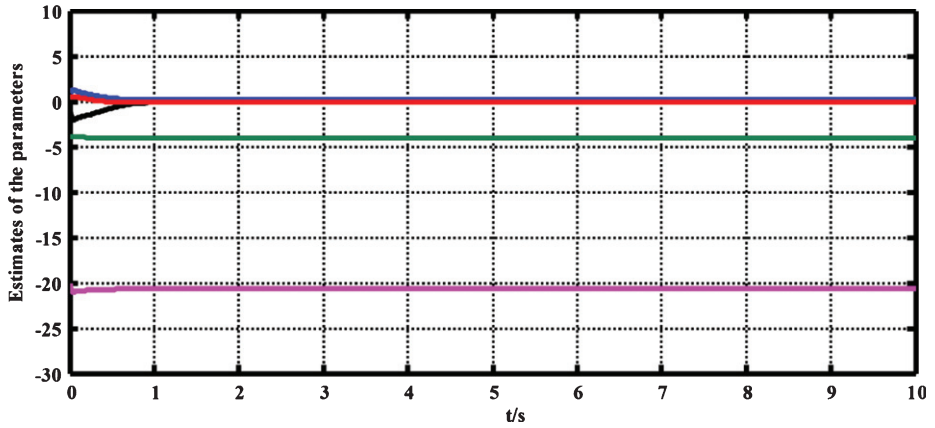

Fig. 10. Estimates of the parameters of $\hat{\theta}_2 + \beta_2$.

shows the mechanical arm controller output. Figure 6(b) shows the tracking of the mechanical arm position. Figure 6(c) and (d) demonstrate the system state x2 and x3, respectively, under the interference output value. As shown in Fig. 6, the output can track the given input under system interference.

Figures 7–10 show the proposed method and traditional methods of dynamic performance, to allow comparative advantages of each method.

Experimental results show that the torque compensation method effectively reduces the nonlinear and time-varying residual vibrations in the robot control system. The torque compensation strategy is a promising technique to suppress the nonlinear and time-varying residual vibrations in 7-DOF humanoid robots because it does not require real-time estimation of vibration frequencies.

5. Conclusion

Humanoid robot arms are a typical nonlinear system; the dynamic performance of the system and the system stability are affected by actuator saturation and the actual control input of the bounded system. A considerable number of studies on trajectory tracking controllers have failed to consider the constraint conditions of the control input saturation. This paper presents and investigates an adaptive fuzzy backstepping scheme that considers the input saturation constraints.

To suppress nonlinear and time-varying residual vibrations in a 7-DOF humanoid robot, a torque compensation method is proposed that calculates torque parameters in real-time by using data from the previous servo cycle.

Based on the Lyapunov method, this paper proposes the adaptive fuzzy backstepping control approach to theoretically suppress the residual vibration of the end-effector in the dual-arm of the humanoid robot. The simulated and experimental results indicate that the torque compensation method effectively reduced the nonlinear and time-varying residual vibrations in the robot control system, and the proposed controller demonstrated asymptotic stability in the entire closed-loop system. As a result, this method can control the dynamic performance of the system and improve the limit of computing power and memory space. In addition, the application of torque compensation is more convenient because this method only requires one step to obtain the torque parameters. Its validity was verified by simulation.

Acknowledgments

This research was supported by the project of new strategic industries of the Chinese Academy of Sciences. We would also like to extend our thanks to our colleagues at the lab for their cooperation on the project. This research was supported by the national key basic research and development program (2014CB744100), and the national nature science foundation of China (No. 51405469).

References

[1] B. Andrea and N. Simaan, Hybrid motion/force control of multi-backbone continuum robots, *The International Journal of Robotics Research* (2015), 0278364915584806.

[2] B.Z. Guo, H.C. Zhou, A.S. Al-Fhaid, et al., Stabilization of Euler-Bernoulli beam equation with boundary moment control and disturbance by active disturbance rejection control and sliding mode control approaches, *Journal of Dynamical & Control Systems* **20**(4) (2014), 539–558.

[3] D. Karagiannis and A. Astolfi, Nonlinear adaptive control of systems in feedback form: An alternative to adaptive backsteeping, *Systems & Control Letters* **57** (2008), 733–739.

[4] G. Rosati, M. Faccio, L. Barbazza, et al., Hybrid fexible assembly systems (H-FAS): Bridging the gap between traditional and fully flexible assembly systems, *The International Journal of Advanced Manufacturing Technology* **81**(5-8) (2015), 1289–1301.

[5] H.C. Huang and C.H. Chiang, Backstepping holonomic tracking control of wheeled robots using an evolutionary fuzzy system with qualified ant colony optimization, *International Journal of Fuzzy Systems* **18**(1) (2016), 28–40.

[6] J.Q. Lou, Y.D. Wei, Y.L. Yang, et al., Hybrid PD and effective multi-mode positive position feedback control for slewing and vibration suppression of a smart flexible manipulator, *Smart Materials and Structures* **24**(3) (2015), 7–21.

[7] J. Zhou and C.Y. Wen, Adaptive backstepping control of uncertain systems: Nonsmooth nonlinearities, *Interactions or Time-Variations*, Springer-Verlag, Berlin Heidelberg, 2008, pp. 189–190.

[8] K.Q. Bai, M.Z. Luo, G.W. Jiang, et al., Research of the torque compensation method for the vibration suppression of the industrial robot, *Proceedings of the 2015 IEEE International Conference on Robotics and Biomimetics*, Zhuhai, China, 2015, pp. 2575–2579.

[9] M.R. Homaeinezhad, I.T. Moghaddam, Z. Khakpour, et al., Short-time linear quadratic form technique for estimating fast-varying parameters in feedback loops, *Asian Journal of Control* **17**(6) (2015), 2289–2302.

[10] S.C. Tong, Y. Li, Y.M. Li, et al., Observer-based adaptive fuzzy backstepping control for a class of stochastic nonlinear strict-feedback systems, *IEEE Transactions on Systems, Man, and Cybernetics, Part B (Cybernetics)* **41**(6) (2011), 1693–1704.

[11] S.C. Tong, Y.M. Li and P. Shi, Observer-based adaptive fuzzy backstepping output feedback control of uncertain MIMO pure-feedback nonlinear systems, *IEEE Transactions on Fuzzy Systems* **20**(4) (2012), 771–785.

[12] S.S. Ge, S. Zhang and W. He, Vibration control of an Euler–Bernoulli beam under unknown spatiotemporally varying disturbance, *International Journal of Control* **84**(5) (2011), 947–960.

[13] W. He, S. Zhang and S.S. Ge, Adaptive boundary control of a nonlinear flexible string system, *IEEE Transactions on Control Systems Technology* **22**(3) (2014), 1088–1093.

[14] B. Xiao, Q.L. Hu and Y.M. Zhang, Adaptive sliding mode fault tolerant attitude tracking control for flexible spacecraft under actuator saturation, *IEEE Transactions on Control Systems Technology* **20**(6) (2012), 1605–1612.